

Development and application of sewage sludge biochar for the removal of methyl red from water environment

Khairunissa Syairah Ahmad Sohaimi^{a,*}, Norissam Nasaru^b, Noor Ainee Zainol^a, Nor Aida Yusoff^a, Nor Munirah Rohaizad^{a,b}, Edza Aria Wikurendra^c, Ayman A. Ghfar^d, Endah Budi Permana Putri^e, Raj Boopathy^f, Achmad Syafiuddin^{c,*}

^aWater Research Group (WAREG), Faculty of Civil Engineering Technology, Universiti Malaysia Perlis, Kompleks Pusat Pengajian Jejawi 3, 02600 Arau, Perlis, Malaysia, emails: syairah@unimap.edu.my (K.S.A. Sohaimi), aineezainol@unimap.edu.my (N.A. Zainol), aidayusoff@unimap.edu.my (N.A. Yusoff), normunirah@unimap.edu.my (N.M. Rohaizad)

^bFaculty of Chemical Engineering Technology, Universiti Malaysia Perlis, Uniciti Alam Campus, Sungai Chuchuh, Padang Besar, 02100, Perlis, Malaysia, email: norissamnasaru02@gmail.com (N. Nasaru)

^cDepartment of Public Health, Universitas Nahdlatul Ulama Surabaya, 60237 Surabaya, Indonesia, emails: achmadsyafiuddin@unusa.ac.id (A. Syafiuddin), edzaaria@unusa.ac.id (E.A. Wikurendra)

^dDepartment of Chemistry, College of Science, King Saud University, P.O. Box: 2455, Riyadh, 11451, Saudi Arabia, email: aghafr@ksu.edu.sa (A.A. Ghfar)

^eInstitute of Research and Community Service (LPPM), Universitas Nahdlatul Ulama Surabaya, 60237 Surabaya, Indonesia, email: endah.budi92@unusa.ac.id (E.B.P. Putri)

^fDepartment of Biological Sciences, Nicholls State University, Thibodaux, LA 70310, USA, email: ramaraj.boopathy@nicholls.edu (R. Boopathy)

Received 30 December 2021; Accepted 16 March 2022

ABSTRACT

Currently, development of an efficient natural adsorbent to remove pollutions becomes crucial since adsorbents derived from chemicals have several shortcomings such as their potential as a new pollution in the environment. Therefore, this study aims to investigate the capability of sewage sludge biochar for the removal of dye. Sewage sludge biochar was synthesized by pyrolysis at different temperatures, which were 350°C, 450°C, 550°C, 650°C, 750°C, and 850°C. The characterization of biochar was conducted by analyzing the percentage yield, ash content, moisture content, Fourier-transform infrared spectroscopy, and pH zero charge. This study found that as the pyrolysis temperature increased, the percentage yield along with moisture content decreased meanwhile the ash content increased. For kinetic studies, pseudo-second-order model gave better result than pseudo-first-order model indicating that adsorption mainly takes place on chemical adsorption. The applicability of adsorption isotherm analyses indicates that the adsorption mechanism followed Freundlich isotherm compared to Langmuir as Freundlich give value of R^2 nearer to 1 (0.9962). It showed that adsorption mechanism behaves in a multi-molecular layer and the adsorption sites are heterogenous on the sewage sludge biochar.

Keywords: Dye removal; Methyl red; Sewage sludge; Adsorption

* Corresponding authors.

1. Introduction

The increasing revolution in science and technology had produced a greater demand for newer chemicals which was used in various industrial activities [1–10]. Organic dyes like methyl red was one of such many new chemicals which used in a lot of industrial processes especially textile, paper, cosmetic and food processing area. The potential toxicity of the dyes and their visibility in surface waters, removal and degradation of the dyes had attracted considerable attention worldwide [11–13]. Textile industry was one of the major industry that contributes mostly to pollution related to dyes [12,14,15]. This was due to its bright colour and ease of application [16–18].

A lot of methods had been used to remove methyl red dyes from aqueous solutions. The methods include hypochlorite treatment, electro-Fenton photocatalytic degradation, adsorption, coagulation, and ozone treatment [19]. The physical method has several limitations such as high energy requirement and high cost [20–22]. On the other hand, chemical methods were not economically feasible due to its high ability and tendency to produce a great quantity of sludge. In current trends recently, much attention had been drawn on the traditional and less problematic method which was known as adsorption [23–25]. Adsorption is considered as promising method because of its high removal efficiency, simple operation, low cost and environmental friendly [23,26–33].

Biochar was known as the potential adsorbent which synthesized by pyrolysis of organic or inorganic materials [34]. In fact, the pyrolyzed product has physicochemical properties suitable for many applications like enhance soil fertility, storage of carbon and also pollutants removal [35]. The quality of biochar produced was dependent on the process operational temperature where the biochar produced at low temperature was compatible on agricultural use due to its availability of nutrients and carbon composition while higher temperature biochar is suitable for adsorbent used for removing contaminants. The biochar that undergoes a high temperature process tends to increase the porosity and this feature was important in removing pollutants [36,37].

Therefore, this study aims to investigate the capability of sewage sludge biochar for the removal of dye. It is noted that the use of sewage sludge biochar to treat methyl red in this study because it has the potential to serve as a lot of pollutants removal agent [38,39]. The use of the sewage sludge from water treatment plant to treat methyl red dyes has been limited in literature. In general, physicochemical properties of sewage sludge biochar produced indicated that this research should be extended on others pollutants removal in the future.

2. Materials and methods

2.1. Feedstock preparation

The sewage sludge that used as feedstock for biochar was obtained from the local water treatment plant at Kuala Perlis, Perlis, Malaysia. Sewage sludge was left to dry in an oven at 105°C for about 24 h to completely remove the moisture. Then, the dried sludge was grinded and sieved

to obtain particles with average size of 250 µm, followed by carbonization at temperatures at 350°C, 450°C, 550°C, 650°C, 750°C, and 850°C in the muffle furnace [40]. The sample was stored in a desiccator prior to the experiment.

2.2. Biochar characterization

Characterization of biochar is performed to choose the best adsorbent for adsorption of methyl red in water by comparing the biochar with different parameters. The five methods were used in biochar characterization were percentage yield, moisture analysis, ash content analysis, Fourier-transform infrared spectroscopy (FTIR) and point of zero charge.

2.2.1. Percentage yield

The percentage yield was done by pyrolyzing raw sewage sludge with 6 different temperatures at 350°C, 450°C, 550°C, 650°C, 750°C, and 850°C. The calculation of percentage yield was done by subtracting the mass of biochar before and the mass of biochar divided by initial mass of biochar after it being burned times by 100 into their respective temperature.

2.2.2. Moisture content

The moisture content of the feedstock was estimated by measuring the weight loss after the drying the samples at 105°C for 2 h. Firstly, the muffle furnace was heated to 300°C to remove moisture on it. Then the porcelain crucible was placed in the heat muffle furnace for about 15 min and then was cooled in the desiccators for 1 h then was weighed. The dried biochar sample was placed in the porcelain crucibles and sent into the oven for about 100°C. After that the crucible was cooled for an hour in desiccator followed by weighing of the crucible.

2.2.3. Ash content

Ash content analysis was performed by determining the mass loss after burned the dried samples in a muffle furnace at 750°C for 3 h. Porcelain crucible with lid was completely removed to achieve complete combustion [41]. Then the crucible was cooled in the desiccator for about 2 h then weighed. After that, the sample were repeatedly be burned in muffle furnace until it got to the point where the loss of ash content is less than 0.0005 g in 1-h period.

2.2.4. FTIR analysis

The FTIR was used to determine and characterize unknown materials (e.g., films, solids, powders, or liquids), identify contamination on or in a material (e.g., particles, fibers, powders, or liquids), identify additives after extraction from a polymer matrix and identify oxidation, decomposition, or uncured monomers in failure analysis investigations. The problem arises when our sample in solid form instead of liquid form hence KBr pellet is used. Potassium bromide (KBr, spectroscopic grade) was typically used as the window material because it is transparent

in the IR from 400–4,000 cm^{-1} . Alternatively, samples can be contained within a KBr matrix and pressed to form a pellet that was then analyzed. Potassium bromide were mixed with the sample biochar at a ratio of 1 mg sample to 10 mg KBr [42]. Then the mixture was crushed to ensure homogeneity and then pressed into a disc for analysis.

2.2.5. pH zero point of charge

Deionized water was added into biochar at the ratio of 1:5 of weight percent in order to analyze the pH of biochar. Then the mixture was whirled to allow it homogeneous for 5 min. After that the initial pH of the solution is measured using pH meter. The zero point of charge of each biochar sample were determined by inserting 50 mL of 0.01 M KNO_3 solution in the conical flask which then adjusted to initial pH between 2 to 11 with 1 M HNO_3 or 1 M NaOH . A 100 mL sealed conical glass with 0.1 g biochar was added with 50 mL aliquot of the 0.01 M KNO_3 . This new mixture was shaken at 150 rpm for 24 h. The final pH obtained by using pH meter. A graph for different pH for both initial and final pH was plotted.

2.3. Methyl red adsorption

The experiment was conducted in batch experiments using 250 mL Erlenmeyer flasks by varying the adsorbent dosage, the pH, the adsorption contact time and the initial concentration of methyl red. Adsorption experiment were done by using the shaker at speed of 100 rpm shaker at 25°C containing 50 mL of methyl red solution and the best biochar from characterization test which is SS650 [40].

2.3.1. Contact time

About 50 mL of the working solution was put in each different conical flask. All the flasks were put in the shaker at 100 rpm and 25°C for a predetermined time period ranging from 20 min to 180 min. Then, flasks were withdrawn from the shaker, solution were centrifuged or filtered, and absorbance of the solutions was measured. A graph was plotted against adsorption capacity vs. contact time.

2.3.2. pH

The effect of pH on the equilibrium uptake of dyes was investigated by employing an initial concentration of MR (100 mg/L) and 0.1 g/50 mL of biochar. The initial pH values were adjusted with 0.1 M HCl or NaOH to form a series of pH from 2 to 10. The suspensions were shaken at room temperature (27°C) using agitation speed (100 rpm), the optimum contact time required to reach the equilibrium (100 min) and the amount of MR adsorbed were determined.

2.3.3. Adsorbent dosage

In this experiment, the effect of adsorbent dosage was being conducted with different doses of biochar which were 0.1, 0.2, 0.3, 0.4 and 0.5 g. In this experiment we are using the chosen biochar which is SS650. Then, series of parameters need be to held constant to give a fair result

throughout the experiment. The experiment was conducted by taking the initial concentration (100 ppm), adsorption contact time (100 min), in 50 mL volume solution with temperature of 30°C at the speed of 100 rpm in optimum pH condition (pH 4).

2.3.4. Initial concentration

The effect of methyl red was studied by analysis of the methyl red removal rate in 20, 40, 60, 80 and 100 ppm. The analysis was performed at room temperature, pH of 4, 100 rpm speed, methyl red initial concentration of with varied ppm and constant adsorbent dosage of optimum value (0.1 g) which obtained from analysis of adsorbent dosage and constant adsorption contact time of optimum value (100 min) which obtained from analysis of adsorption contact time with 50 mL of methyl red sample solution.

2.4. Adsorption kinetic

Several models were used to fit experiment data for adsorption kinetics identification. Methyl red adsorption dynamic processes were studied by pseudo-first-order and pseudo-second-order models. These two models describe the solute uptake rate at solid-solution interface and control the resident time of adsorbate and possibilities of desorption. The analysis was using the result from the adsorption capacity against contact time. The linear form of pseudo-first-order model and pseudo-second-order models are shown below.

$$\text{Pseudo-first-order: } \log(Q_e - Q_t) = \log Q_e - \left(\frac{k_1}{2.303} \right) t \quad (1)$$

$$\text{Pseudo-second-order: } \frac{t}{Q_t} = \frac{1}{k_2 Q_e} + \frac{t}{Q_e} \quad (2)$$

2.5. Adsorption isotherm

Langmuir isotherms model assumes the existence of a monolayer adsorption with homogeneity of the surface. Freundlich isotherm model assumes that adsorption occurs on a heterogeneous surface with interaction between adsorbed molecules. The analysis was using the result from the adsorption capacity against initial concentration. The adsorption kinetic and adsorption isotherm model were calculated by using the formula shown below.

$$\text{Langmuir: } \frac{C_e}{Q_e} = \frac{1}{Q_m} + \frac{1}{Q_m} C_e \quad (3)$$

$$\text{Freundlich: } \ln Q = \ln K_f + \frac{\ln C_e}{n} \quad (4)$$

3. Results and discussions

3.1. Biochar characterization

There are many characterization analyses of physical and chemical properties of biochar produced by pyrolysis

like percentage yield, moisture content analysis, ash content analysis, FTIR and pH zero point of charge analysis. The characterization was being observed and analysed to select the most effective biochar sample for methyl red adsorption on sewage sludge biochar.

Percentage yield was performed onto the sewage sludge biochar which were pyrolyzed at different temperatures of 350°C, 450°C, 550°C, 650°C, 750°C, and 850°C that were categorized as SS350, SS450, SS550, SS650, SS750 and SS850, respectively. It is observed that SS850 tabulate the lowest percentage yield at 82.8% while SS350 recorded the highest percentage yield at 95.55%. It is also observed that the reading of percentage yield display descending patterns where the reading of percentage yield become decrease when the biochar temperature increased. This can be shown by the percentage yield of SS450, SS550, SS650, SS750 where they recorded a percentage yield of 91.5%, 90.42%, 85.49% and 83.86% respectively. As shown in Fig. 1, increasing temperature resulted in reduction in yield of biochar and this reduction may be due to rapid reduction of oxygen (O), hydrogen (H) and volatiles content at high temperature [43].

In this study, the moisture content was observed in sewage sludge biochar with 5 different pyrolysis temperature which is 350°C, 450°C, 550°C, 650°C, 750°C, and 850°C namely SS350, SS450, SS550, SS650, SS750, SS850, respectively. It was found out that the percentage moisture was the lowest at SS650 (0.09%) followed by SS750 (0.49%) and SS850 (1.22%). Meanwhile the highest moisture recorded at lower temperature which is SS450 (57.53%) followed by

SS350 (1.9%) and SS550 (1.51%). It is concluded that lower pyrolysis temperature recorded the higher moisture content while the higher pyrolysis temperature recorded the lower moisture content. This can be explained by the losses in (water content) moisture content for higher pyrolysis temperature where in high temperature the rate of drying of biochar samples also increased significantly along the process. Hence, it was concluded that SS650 was the optimum biochar due to its lower moisture content.

The different pyrolysis biochar temperature was performed for determination of the ash content at a fixed heating temperature of 750°C for 6 h. From Fig. 2, it is observed that SS350 tabulate the lowest percentage of ash content at 65.83% while SS850 recorded the highest ash content percentage at 97.39%. It is also observed that the reading of percentage ash content is directly proportional to the biochar temperature where the reading of percentage ash content become increased when the biochar temperature increased. A study by Callegari and Capodaglio [44] show that the increase in ash content is followed with the increasing pyrolysis temperature. Such increase is a typical tendency for sewage sludge (and other feedstock) chars, due to the concentration of the non-volatile mineral constituents that form the ash, and the removal of volatile organic decomposition products. Mineral fractions are, in fact, dominant in both untreated sewage sludges and chars, usually much higher than in (bio)chars derived from other materials. In this experiment, SS650 was chosen as the best biochar as it presents the criteria of being the best biochar which is having the lower moisture content and lower ash content.

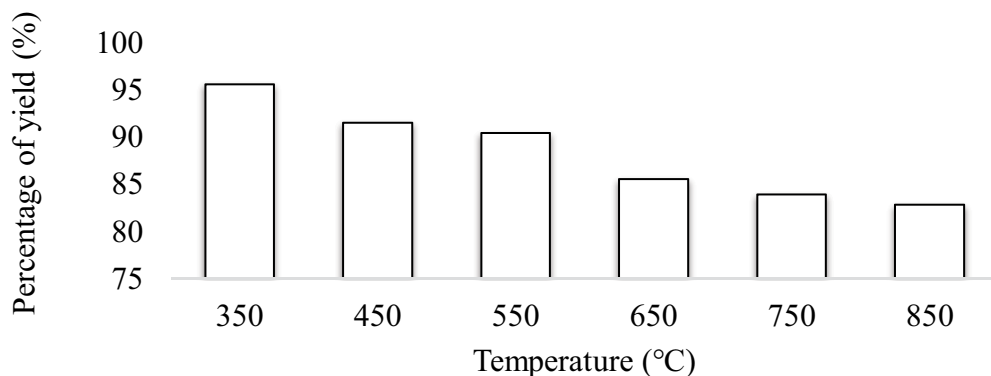


Fig. 1. Percentage of yield of SS350, SS450, SS550, SS650, SS750, and SS850.

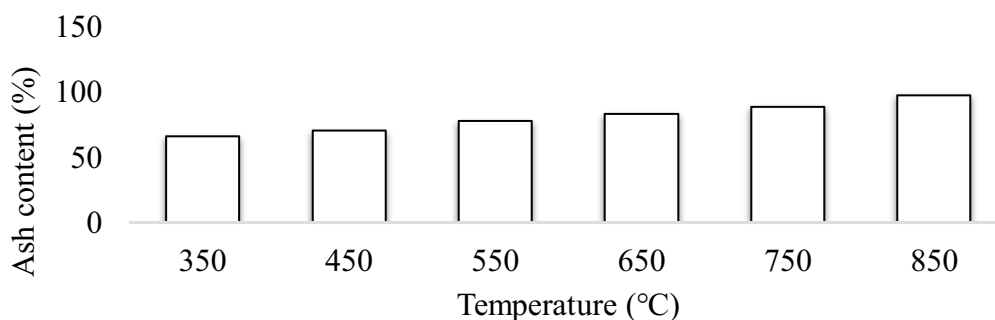


Fig. 2. Percentage ash content of SS350, SS450, SS550, SS650, SS750 and SS850.

Based on Fig. 3, it is found out that the functional groups that exist within the spectra of sewage sludge biochar were conjugated aldehydes, alkene and sulfoxide. The first wave number would be the indication of conjugated aldehydes with wavelength of $1,685.9\text{ cm}^{-1}$. The vibration mode was very strong in C=O stretching at the range wavenumber of $1,710\text{--}1,685\text{ cm}^{-1}$. The second wave in the diagram spectra would be the presence indication of sulfoxide, a common pollutant that exist in typical sludges. It projected a wavelength of 1059.3 with strong vibration mode in between S=O stretching within the range of $1,070\text{--}1,030\text{ cm}^{-1}$ wavenumber. The final functional would be alkene. It projected the wavelength of 804.28 cm^{-1} with a strong vibration mode on C=C bending within the range of $(840\text{--}790\text{ cm}^{-1})$. The functional group that are mainly responsible for the adsorption process are the sulfinyl(sulfoxide) and carbonyl(aldehyde). At low pH (pH 4–5), the surface functional groups are being protonated thus a positive charge would be formed on the surface. In acidic medium, these two functional group carried positive charge on the adsorbent surface resulting in electrostatic interaction between negatively charged carboxyl group that exist on methyl red.

It is found out that the pH zero point of charge of biochar samples lies almost on pH 5. This indicates that the pH zero charge of biochar samples on mild acidic condition. Therefore, in this study mild acidic pH which is between 4 and 5 was used as the pH that maximizes the adsorption capacity of sewage sludge biochar. This methyl red was adsorbed onto sewage sludge biochar as methyl red was anionic and the surface sewage sludge biochar was positively charge in mild acidic condition. (Bio)char surface that is positively charged in the lower pH range (mild acid) which is when $\text{pH} < \text{pH}_0$ (point of zero charge) allows anionic dye to be easily captured due to the electrostatic interaction [44].

3.2. Adsorption process

In this study, there were 4 parameters that were evaluated on removing methyl red using sewage sludge biochar which were known as adsorbent dosage, adsorption contact time, adsorption initial concentration and the effect of pH. Based on Fig. 4, the adsorption capacity displays a distinctive pattern which the reading was decreased from 31.53 to 9.56 mg/g as the adsorbent dosage increases from 0.1 to 0.5 g . It was concluded that the highest adsorption capacity was recorded at adsorbent dosage of 0.1 g . The increased in the adsorption capacity was due to the increase in the adsorbent mass that can increase the availability more binding site for adsorption. However, further increased in adsorbent mass from 0.2 to 0.5 g had decreased the adsorption capacity. This is due to unavailability of the adsorbate sites that are fully saturated by the methyl red dye molecules. When more biochar is added to the process, the binding site become the limiting factor as the adsorption progress. As time passes when the binding site are fully equipped, here where the adsorption stops and reaches the plateau. According to Kuang et al. [45], they had studied that when an adsorbent quantity was being increased, they found difficulty on aiding to the scarce of binding site in the long run. These was led to a decrease in the adsorption capacity of the biochar.

It indicates that adsorption capacity of methyl red was directly proportional as the adsorption capacity increases as the initial concentration was being increased from 20 to 100 ppm . The lowest adsorption capacity was at the concentration of 20 ppm while the highest recorded reading of adsorption capacity at the concentration of 100 ppm . This can be explained by the concept of mass transfer and equilibrium. Higher concentration resulted in a higher driving force of the concentration gradient. This driving force accelerated the diffusion of dye from the solution into the

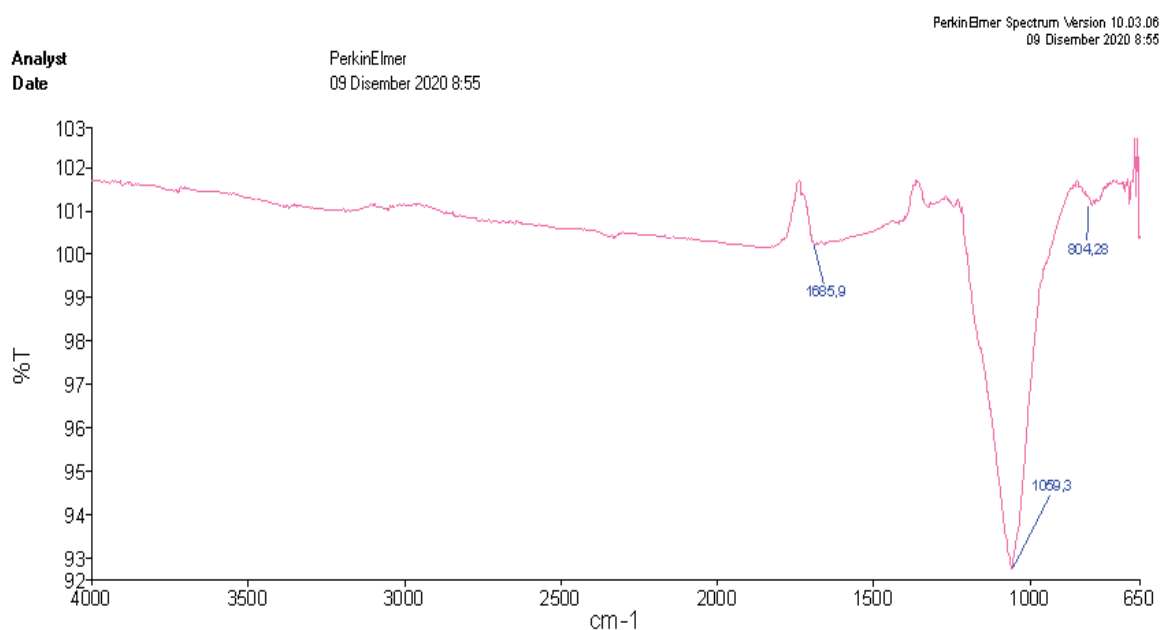


Fig. 3. FTIR analysis.

adsorbent. These observations can be explained by the fact that enough adsorption sites are available to accommodate an increasing number of dye molecules.

According to Silva et al. [46], as the sewage sludge biochar surface is negatively charged at high pH, a significantly strong electrostatic attraction appears between the negatively charged carbon surface and cationic dye molecule leading to maximum adsorption of methyl red dyes. Moreover, the increasing in the adsorption of MR with decreasing of pH value is also due to the attraction between methyl red dye and excess H^+ ions in the solution. Meanwhile when the adsorption capacity decreases at basic pH (8–11) this was mostly due to the dominance of the negative charges at the surface of the adsorbent or due to the low competition of OH^- and dye anions in basic pH [47]. As shown in Fig. 5, pH 2 is the optimum pH for methyl red adsorption, however, pH4 has been selected the optimum condition as it still acidic solution and only has slight difference with adsorption capacity that achieved in pH 2. Also, it is supported by results from ph zero charge analysis which ph4 is the best ph condition for methyl red adsorption by sewage sludge biochar.

The rapid adsorption at the initial contact time is due to the highly negatively charged surface of the sewage sludge biochar for adsorption of methyl red in the solution at pH 4–5. Later slow rate of MR adsorption is probably due to the electrostatic hindrance or repulsion between the adsorbed negatively charged adsorbate species onto the surface of sewage sludge biochar and the available adsorbate species in the solution as well as the slow pore diffusion of the solute ions into the bulk of the adsorbent [48,49]. The equilibrium was achieved at 100 min when the maximum methyl red adsorption onto sewage sludge biochar due to the constant reading of adsorption capacity or what we called the plateau stages.

3.3. Adsorption kinetic

Figs. 6 and 7 illustrate the graph of pseudo-first-order model and pseudo-second-order model. Both graphs display different patterns which Fig. 6 the relationship was inversely proportional while Fig. 7 displays a direct proportional reading. It was observed that pseudo-second-order model gives a better value of correlation coefficient R^2 which

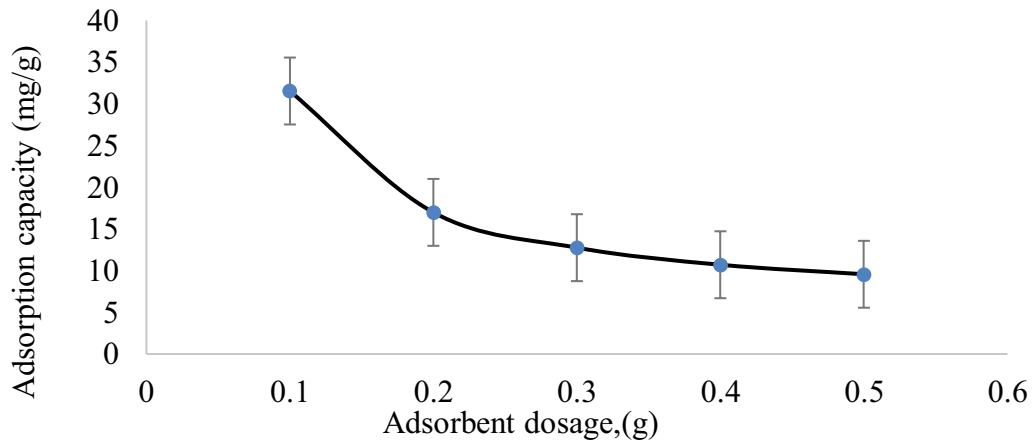


Fig. 4. Adsorption capacity at different adsorbent dose.

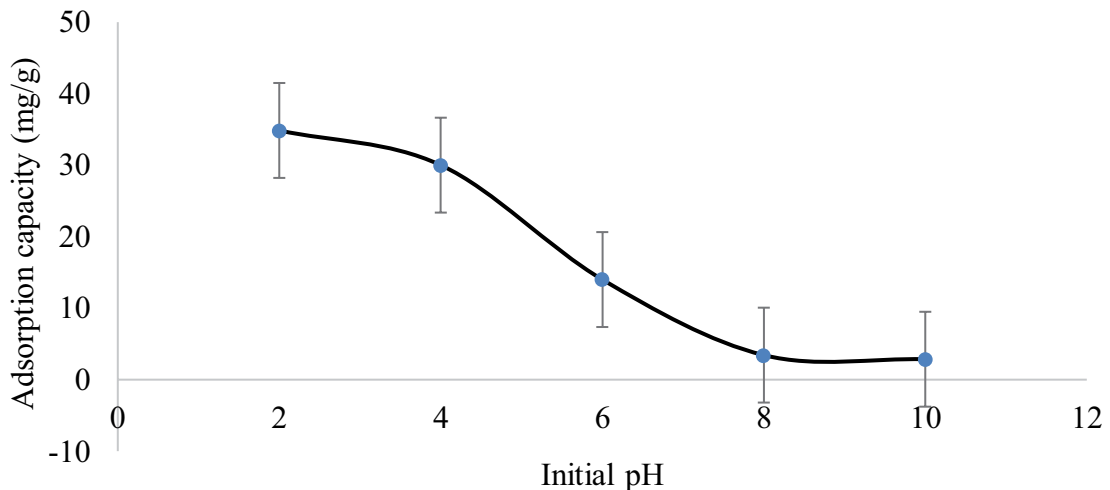


Fig. 5. Adsorption capacity at different initial pH.

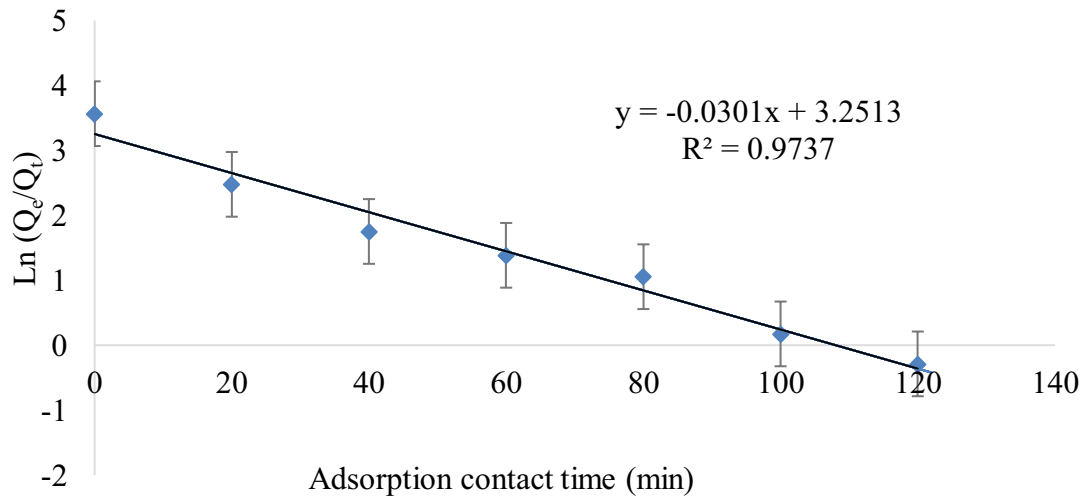


Fig. 6. Pseudo-first-order model, $\ln(Q_e - Q_t)$ against adsorption contact time (min).

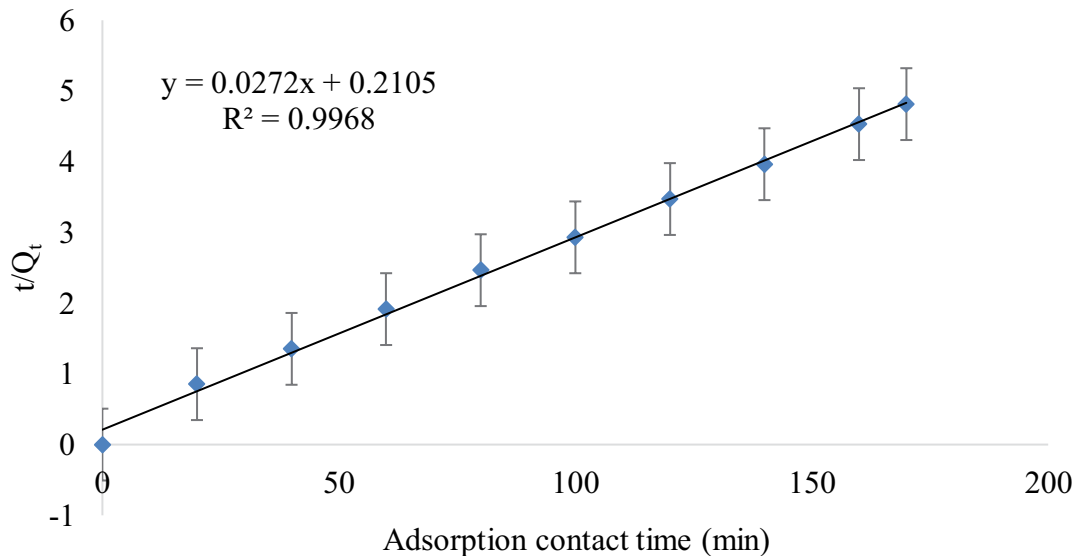


Fig. 7. Pseudo-second-order model, t/Q_t against adsorption contact time (min).

the value was almost near to 1 (0.9968) compared to pseudo-first-order model (0.9737). This shows that the adsorption of methyl red onto sewage sludge biochar is a second-order reaction. This can be concluded that adsorption process was being controlled by chemical adsorption (pseudo-second-order) mechanism instead of physical adsorption (pseudo-first-order) [20]. It is also supported by effect of pH on methyl red adsorption process which shown better performance at acidic than basic condition. Thus, there has adsorption mechanism of chemical electrostatic attraction appears between the negatively charged carbon surface and cationic dye molecule.

3.4. Adsorption isotherm

The correlation coefficients reported in Freundlich isotherm showed strong positive evidence on the adsorption of MR onto sewage sludge biochar which the value of R^2 was

near to 1 which is 0.9962 as shown in Fig. 8. The adsorption feature was determined with how close the value of correlation coefficient of R^2 with 1, hence from the experiment we can observe that Freundlich model was the best fitting model for adsorption as the value of R^2 is 0.9962 compared to Freundlich which the value of R^2 was 0.8752. This indicates that methyl red adsorption corresponds heterogeneously to the complete multilayer coverage on the adsorbent surface [41].

4. Conclusions

The aim of this study was to investigate the capability of sewage sludge biochar for the removal of dye. Based on the characterization, SS650 was selected as the biochar because it has lower moisture content and lower ash content compared to others. FTIR analysis revealed that SS650 contains conjugated aldehydes, alkene and a common substance

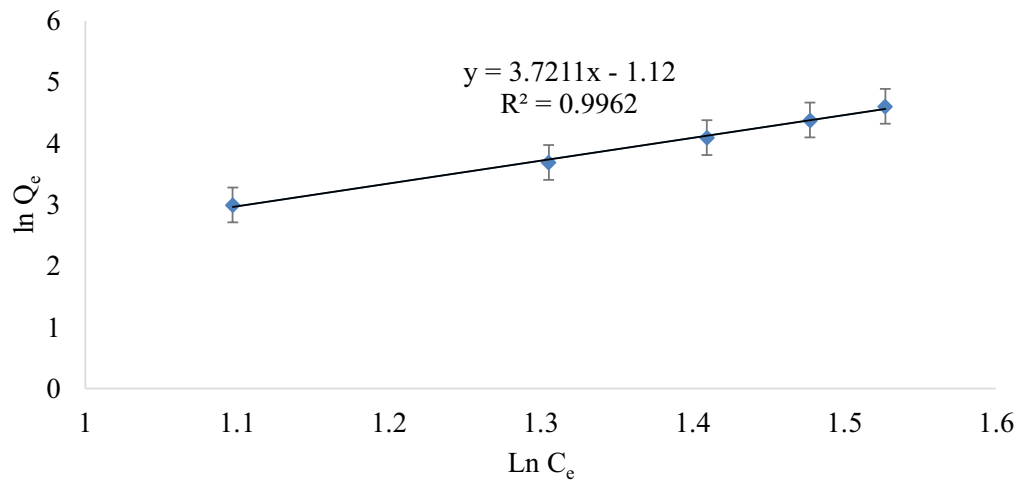


Fig. 8. Freundlich isotherm, $\ln Q_e$ against $\ln C_e$.

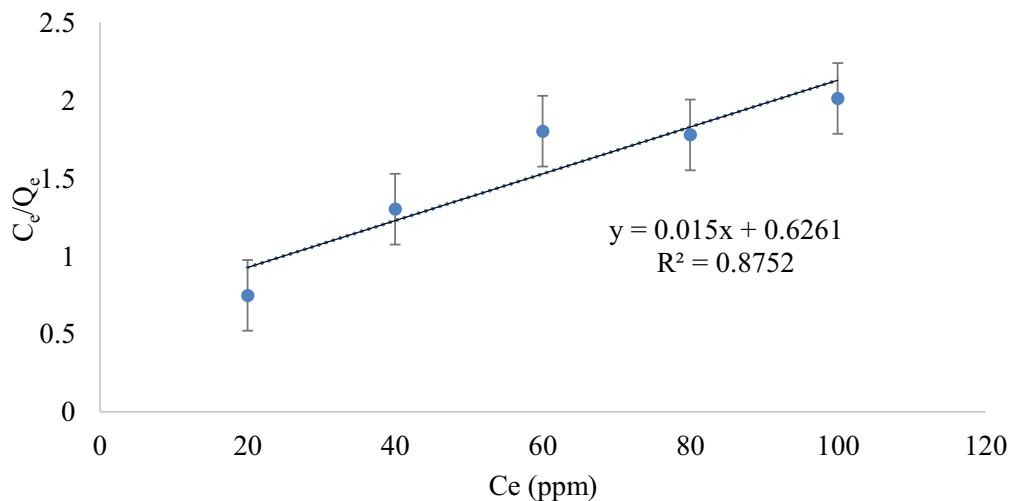


Fig. 9. Langmuir isotherm, C_e/Q_e against equilibrium concentrations, C_e (ppm).

found in typical sludges which was sulfoxide. The pH zero charge had indicated that the most optimum pH for sewage sludge adsorption falls under mild acidic pH which was between the range of 4–5. The maximum adsorption capacity of SS650 biochar was recorded at 31.35 mg/g at optimum dosage of 0.1 g. The kinetic studies had shown that methyl red relies mainly on chemical adsorption due to its greater correlation coefficient that followed the pseudo-second-order model with greater value of R^2 (0.9968). The Freundlich isotherm were the best fit compared to Langmuir isotherm as Freundlich give value of R^2 that is near to 1 which is 0.9962. This indicates that the adsorption works on multilayer heterogeneously on adsorbent surface.

Acknowledgments

The authors would like to express the greatest appreciation to the Department of Chemical Engineering Technology, Faculty of Chemical Engineering Technology (FTKK), Financial support from Research Materials Fund (RESMATE)

(9001-00630) and Water Research Group (WAREG). The authors are grateful to the Researchers Supporting Project number (RSP-2021/407), King Saud University, Riyadh, Saudi Arabia for the financial support.

Conflicts of interest

The authors declare no conflict of interest.

References

- [1] G. Sharma, Mu. Naushad, Adsorptive removal of noxious cadmium ions from aqueous medium using activated carbon/zirconium oxide composite: isotherm and kinetic modelling, *J. Mol. Liq.*, 310 (2020) 113025, doi: 10.1016/j.molliq.2020.113025.
- [2] G. Sharma, B. Thakur, A. Kumar, S. Sharma, Mu. Naushad, F.J. Stadler, Atrazine removal using chitin-*cl*-poly(acrylamide-co-itaconic acid) nanohydrogel: isotherms and pH responsive nature, *Carbohydr. Polym.*, 241 (2020) 116258, doi: 10.1016/j.carbpol.2020.116258.
- [3] F. Abdullah, N.A.F. Salleh, M.L. Selahuddeen, Phytochemical and toxicity analysis of *Leucas zeylanica* crude extracts, *Environ. Toxicol. Manage.*, 1 (2021) 1–8.

- [4] A.A.M. Akahir, Z.M. Lazim, S. Salmiati, Removal of silver nanoparticles using phytoremediation method, *Environ. Toxicol. Manage.*, 1 (2021) 28–31.
- [5] T. Hadibarata, B.V. Tangahu, Green engineering principles and application: bioremediation, *Environ. Toxicol. Manage.*, 1 (2021) 1–8.
- [6] K.N. Mahmud, T.H. Wen, Z.A. Zakaria, Activated carbon and biochar from pineapple waste biomass for the removal of methylene blue, *Environ. Toxicol. Manage.*, 1 (2021) 30–36.
- [7] N.S. Zaidi, J. Sohaili, Z.Z. Loh, A. Arisa, N. Hussein, Effect of metal content from sewage sludge on the growth of *Orthosiphon stamineus*, *Environ. Toxicol. Manage.*, 1 (2021) 29–34.
- [8] A. Shahid, M. Usman, Z. Atta, S.G. Musharraf, S. Malik, A. Elkamel, M. Shahid, N. Abdulhamid Alkhattabi, M. Gull, M.A. Mehmood, Impact of wastewater cultivation on pollutant removal, biomass production, metabolite biosynthesis, and carbon dioxide fixation of newly isolated cyanobacteria in a multiproduct biorefinery paradigm, *Bioresour. Technol.*, 333 (2021) 125194, doi: 10.1016/j.biortech.2021.125194.
- [9] F. Khan, A. Shahid, H. Zhu, N. Wang, M.R. Javed, N. Ahmad, J. Xu, M.A. Alam, M.A. Mehmood, Prospects of algae-based green synthesis of nanoparticles for environmental applications, *Chemosphere*, 293 (2022) 133571, doi: 10.1016/j.chemosphere.2022.133571.
- [10] A. Shahid, A.Z. Khan, S. Malik, C.-G. Liu, M.A. Mehmood, A. Syafiuddin, N. Wang, H. Zhu, R. Boopathy, Advances in green technologies for the removal of effluent organic matter from the urban wastewater, *Curr. Pollut. Rep.*, 7 (2021) 463–475.
- [11] A.I. Abd-Elhamid, M. Emran, M.H. El-Sadek, A.A. El-Shanshory, H.M.A. Soliman, M.A. Akl, M. Rashad, Enhanced removal of cationic dye by eco-friendly activated biochar derived from rice straw, *Appl. Water Sci.*, 10 (2020) 45, doi: 10.1007/s13201-019-1128-0.
- [12] G. Sharma, A. Kumar, S. Sharma, Mu. Naushad, P. Dhiman, D.-V.N. Vo, F.J. Stadler, Fe₃O₄/ZnO/Si₃N₄ nanocomposite based photocatalyst for the degradation of dyes from aqueous solution, *Mater. Lett.*, 278 (2020) 128359, doi: 10.1016/j.matlet.2020.128359.
- [13] G. Sharma, D.D. Dionysiou, S. Sharma, A. Kumar, A.H. Al-Muhtaseb, Mu. Naushad, F.J. Stadler, Highly efficient Sr/Ce/activated carbon bimetallic nanocomposite for photoinduced degradation of rhodamine B, *Catal. Today*, 335 (2019) 437–451.
- [14] Mu. Naushad, G. Sharma, Z.A. Allothman, Photodegradation of toxic dye using Gum Arabic-crosslinked-poly(acrylamide)/Ni(OH)₂/FeOOH nanocomposites hydrogel, *J. Cleaner Prod.*, 241 (2019) 118263, doi: 10.1016/j.jclepro.2019.118263.
- [15] D.N. Ahmed, L.A. Naji, A.A.H. Faisal, N. Al-Ansari, Mu. Naushad, Waste foundry sand/MgFe-layered double hydroxides composite material for efficient removal of Congo red dye from aqueous solution, *Sci. Rep.*, 10 (2020) 2042, doi: 10.1038/s41598-020-58866-y.
- [16] S. Wong, N.A. Ghafar, N. Ngadi, F.A. Razmi, I.M. Inuwa, R. Mat, N.A.S. Amin, Effective removal of anionic textile dyes using adsorbent synthesized from coffee waste, *Sci. Rep.*, 10 (2020) 2928, doi: 10.1038/s41598-020-60021-6.
- [17] A. Syafiuddin, M.A. Fulazzaky, Decolorization kinetics and mass transfer mechanisms of Remazol Brilliant Blue R dye mediated by different fungi, *Biotechnol. Rep.*, 29 (2021) e00573, doi: 10.1016/j.btre.2020.e00573.
- [18] A. Syafiuddin, R. Boopathy, Role of anaerobic sludge digestion in handling antibiotic resistant bacteria and antibiotic resistance genes – a review, *Bioresour. Technol.*, 330 (2021) 124970, doi: 10.1016/j.biortech.2021.124970.
- [19] A. Ratnasari, A. Syafiuddin, R. Boopathy, S. Malik, M. Aamer Mehmood, R. Amalia, D. Dwi Prastyo, N. Syamimi Zaidi, Advances in pretreatment technology for handling the palm oil mill effluent: challenges and prospects, *Bioresour. Technol.*, 344 (2022) 126239, doi: 10.1016/j.biortech.2021.126239.
- [20] T. Hadibarata, X.K. Chia, Cleaner production: a brief review on definitions, trends and the importance in environment protection, *Environ. Toxicol. Manage.*, 1 (2021) 23–27.
- [21] T. Hadibarata, B.A. Permatasari, Groundwater and society: fresh submarine groundwater discharge and its management improvement, *Environ. Toxicol. Manage.*, 1 (2021) 19–22.
- [22] M.N.H. Jusoh, C.N. Yap, T. Hadibarata, H. Jusoh, M.Z.M. Najib, Nanomaterial for inorganic pollutant remediation, *Environ. Toxicol. Manage.*, 1 (2021) 18–25.
- [23] A. Syafiuddin, S. Salmiati, J. Jonbi, M.A. Fulazzaky, Application of the kinetic and isotherm models for better understanding of the behaviors of silver nanoparticles adsorption onto different adsorbents, *J. Environ. Manage.*, 218 (2018) 59–70.
- [24] M.A. Fulazzaky, N.A.A. Salim, M.H. Khamidun, M.H. Puteh, A.R.M. Yusoff, N.H. Abdullah, A. Syafiuddin, M.A.A. Zaini, The mechanisms and kinetics of phosphate adsorption onto iron-coated waste mussel shell observed from hydrodynamic column, *Int. J. Environ. Sci. Technol. (Tehran)*, (2021), doi: 10.1007/s13762-021-03563-0.
- [25] A. Syafiuddin, M.A. Fulazzaky, S. Salmiati, A.B.H. Kueh, M. Fulazzaky, M.R. Salim, Silver nanoparticles adsorption by the synthetic and natural adsorbent materials: an exclusive review, *Nanotechnol. Environ. Eng.*, 5 (2020) 1–18.
- [26] D. Phuong, N. Loca, T. Miyaniishi, Efficiency of dye adsorption by biochars produced from residues of two rice varieties, Japanese Koshihikari and Vietnamese IR50404, *Desal. Water Treat.*, 165 (2019) 333–351.
- [27] T. Hadibarata, A. Syafiuddin, F.A. Al-Dhabaan, M.S. Elshikh, Rubiyatno, Biodegradation of Mordant orange-1 using newly isolated strain *Trichoderma harzianum* RY44 and its metabolite appraisal, *Bioprocess Biosyst. Eng.*, 41 (2018) 621–632.
- [28] A. Syafiuddin, S. Salmiati, T. Hadibarata, A.B.H. Kueh, M.R. Salim, M.A.A. Zaini, Silver nanoparticles in the water environment in Malaysia: Inspection, characterization, removal, modeling, and future perspective, *Sci. Rep.*, 8 (2018) 1–15.
- [29] D.A. Al Farraj, T. Hadibarata, A. Yuniarto, A. Syafiuddin, H.K. Surtikanti, M.S. Elshikh, M.M. Al Khulaifi, R. Al-Kufaidy, Characterization of pyrene and chrysenes degradation by halophilic *Hortaea* sp. B15, *Bioprocess Biosyst. Eng.*, 42 (2019) 963–969.
- [30] A.A.-F. Mostafa, M.S. Elshikh, A.A. Al-Askar, T. Hadibarata, A. Yuniarto, A. Syafiuddin, Decolorization and biotransformation pathway of textile dye by *Cylindrocephalum aurelium*, *Bioprocess Biosyst. Eng.*, 42 (2019) 1483–1494.
- [31] A. Syafiuddin, S. Salmiati, T. Hadibarata, M.R. Salim, A.B.H. Kueh, S. Suhartono, Removal of silver nanoparticles from water environment: experimental, mathematical formulation, and cost analysis, *Water Air Soil Pollut.*, 230 (2019) 102–117.
- [32] A. Ratnasari, A. Syafiuddin, A.B.H. Kueh, S. Suhartono, T. Hadibarata, Opportunities and challenges for sustainable bioremediation of natural and synthetic estrogens as emerging water contaminants using bacteria, fungi, and algae, *Water Air Soil Pollut.*, 232 (2021) 242, doi: 10.1007/s11270-021-05183-3.
- [33] A. Ratnasari, N.S. Zaidi, A. Syafiuddin, R. Boopathy, A.B.H. Kueh, R. Amalia, D.D. Prasetyo, Prospective biodegradation of organic and nitrogenous pollutants from palm oil mill effluent by acidophilic bacteria and archaea, *Bioresour. Technol. Rep.*, 15 (2021) 100809, doi: 10.1016/j.biteb.2021.100809.
- [34] P. Ganguly, R. Sarkhel, P. Das, Synthesis of pyrolyzed biochar and its application for dye removal: batch, kinetic and isotherm with linear and non-linear mathematical analysis, *Surf. Interfaces*, 20 (2020) 100616, doi: 10.1016/j.surfin.2020.100616.
- [35] A. Mohammadi, B. Khoshnevisan, G. Venkatesh, S. Eskandari, A critical review on advancement and challenges of biochar application in paddy fields: environmental and life cycle cost analysis, *Processes*, 8 (2020) 1275, doi: 10.3390/pr8101275.
- [36] C.C. de Figueiredo, A. de Souza Prado Junqueira Reis, A.S. de Araujo, L.E.B. Blum, K. Shah, J. Paz-Ferreiro, Assessing the potential of sewage sludge-derived biochar as a novel phosphorus fertilizer: influence of extractant solutions and pyrolysis temperatures, *Waste Manage.*, 124 (2021) 144–153.
- [37] S. Wei, M. Zhu, X. Fan, J. Song, P. Peng, K. Li, W. Jia, H. Song, Influence of pyrolysis temperature and feedstock on carbon fractions of biochar produced from pyrolysis of rice straw,

- pine wood, pig manure and sewage sludge, *Chemosphere*, 218 (2019) 624–631.
- [38] A.N. Matheri, N.S. Eloko, F. Ntuli, J.C. Ngila, Influence of pyrolyzed sludge use as an adsorbent in removal of selected trace metals from wastewater treatment, *Case Stud. Chem. Environ. Eng.*, 2 (2020) 100018, doi: 10.1016/j.cscee.2020.100018.
- [39] B.A. Militaru, R. Pode, L. Lupa, W. Schmidt, A. Tekle-Röttering, N. Kazamer, Using sewage sludge ash as an efficient adsorbent for Pb(II) and Cu(II) in single and binary systems, *Molecules*, 25 (2020) 2559, doi: 10.3390/molecules25112559.
- [40] K.S.A. Sohaimi, N. Ngadi, H. Mat, I.M. Inuwa, S. Wong, Synthesis, characterization and application of textile sludge biochars for oil removal, *J. Environ. Chem. Eng.*, 5 (2017) 1415–1422.
- [41] D. Aller, S. Bakshi, D.A. Laird, Modified method for proximate analysis of biochars, *J. Anal. Appl. Pyrolysis*, 124 (2017) 335–342.
- [42] M.S. Hasan, R. Vasquez, M. Geza, Application of biochar in stormwater treatment: experimental and modeling investigation, *Processes*, 9 (2021) 860, doi: 10.3390/pr9050860.
- [43] S.-X. Zhao, N. Ta, X.-D. Wang, Effect of temperature on the structural and physicochemical properties of biochar with apple tree branches as feedstock material, *Energies*, 10 (2017) 1293, doi: 10.3390/en10091293.
- [44] A. Callegari, A.G. Capodaglio, Properties and beneficial uses of (bio)chars, with special attention to products from sewage sludge pyrolysis, *Resources*, 7 (2018) 20, doi: 10.3390/resources7010020.
- [45] Y. Kuang, X. Zhang, S. Zhou, Adsorption of methylene blue in water onto activated carbon by surfactant modification, *Water*, 12 (2020) 587, doi: 10.3390/w12020587.
- [46] C.E. de Farias Silva, B.M.V. da Gama, A.H. da Silva Gonçalves, J.A. Medeiros, A.K. de Souza Abud, Basic-dye adsorption in albedo residue: effect of pH, contact time, temperature, dye concentration, biomass dosage, rotation and ionic strength, *J. King Saud Univ. – Eng. Sci.*, 32 (2020) 351–359.
- [47] I.A. Ahmed, A.H. Ragab, M.A. Habila, T.S. Alomar, E.H. Aljuhani, Equilibrium and kinetic study of anionic and cationic pollutants remediation by limestone–chitosan–alginate nanocomposite from aqueous solution, *Molecules*, 26 (2021) 2586, doi: 10.3390/molecules26092586.
- [48] C.S. Nkutha, N.D. Shooto, E.B. Naidoo, Adsorption studies of methylene blue and lead ions from aqueous solution by using mesoporous coral limestones, *S. Afr. J. Chem. Eng.*, 34 (2020) 151–157.
- [49] C. Santhosh, E. Daneshvar, K.M. Tripathi, P. Baltrėnas, T. Kim, E. Baltrėnaitė, A. Bhatnagar, Synthesis and characterization of magnetic biochar adsorbents for the removal of Cr(VI) and Acid orange 7 dye from aqueous solution, *Environ. Sci. Pollut. Res.*, 27 (2020) 32874–32887.

Author Query

AQ1

Inline text citation for the Figure 9 is missing. Kindly provide the same.